MATHEMATICAL BIOSCIENCES
AND ENGINEERING
Volume **5**, Number **2**, April **2008**

http://www.mbejournal.org/

pp. **239–260**

"TRAVELING WAVE" SOLUTIONS OF FITZHUGH MODEL WITH CROSS-DIFFUSION

Faina Berezovskaya

Department of Mathematics, Howard University
Washington D.C., 20059, USA

Erika Camacho

Department of Mathematical Sciences and Applied Computing, Arizona State University
Glendale, AZ 85306, USA

Stephen Wirkus

Department of Mathematical Sciences and Applied Computing, Arizona State University
Glendale, AZ 85306, USA

Georgy Karev

National Centre for Biotechnological Information, National Institutes of Health
Bethesda, MD 20894, USA

(Communicated by Sharon Crook)

Abstract. The FitzHugh-Nagumo equations have been used as a caricature of the Hodgkin-Huxley equations of neuron firing and to capture, qualitatively, the general properties of an excitable membrane. In this paper, we utilize a modified version of the FitzHugh-Nagumo equations to model the spatial propagation of neuron firing; we assume that this propagation is (at least, partially) caused by the cross-diffusion connection between the potential and recovery variables. We show that the cross-diffusion version of the model, besides giving rise to the typical fast traveling wave solution exhibited in the original "diffusion" FitzHugh-Nagumo equations, additionally gives rise to a slow traveling wave solution. We analyze all possible traveling wave solutions of the model and show that there exists a threshold of the cross-diffusion coefficient (for a given speed of propagation), which bounds the area where "normal" impulse propagation is possible.

1. **Introduction.** Hodgkin, Huxley, and Katz in the 1940s explored experimentally and mathematically the nature of nerve impulses. Their work revealed that the electrical pulses across the membrane arise from the uneven distribution between the intracellular fluid and the extracellular fluid of potassium (K^+), sodium (Na^+), and protein anions (see [34] for details). This entire process of rapid change in potential from threshold to peak reversal and then back to the resting potential level is called an *action potential*, impulse, or spike (see schematic diagram in Fig. 1). The process was mathematically investigated by Hodgkin and Huxley in 1952 with a four-variable model [19]. In 1961 FitzHugh proposed a simplified two-variable model of an excitable membrane, which made it possible to illustrate the various

2000 *Mathematics Subject Classification.* Primary: 34C20, 34C23,; Secondary: 92C99.
Key words and phrases. FitzHugh, traveling wave solutions, cross-diffusion.
The first author is supported in part by NSF Grant #HRD0401697.

physiological states involved in an action potential (such as resting, active, refractory, enhanced, and depressed) in the phase plane (see [12]). The FitzHugh system, although a caricature of the Hodgkin-Huxley four equations, captures much of the same dynamical behavior and, in particular, demonstrates the spike-like behavior (see Section 2 and Figs. 2, 3, 7, 8).

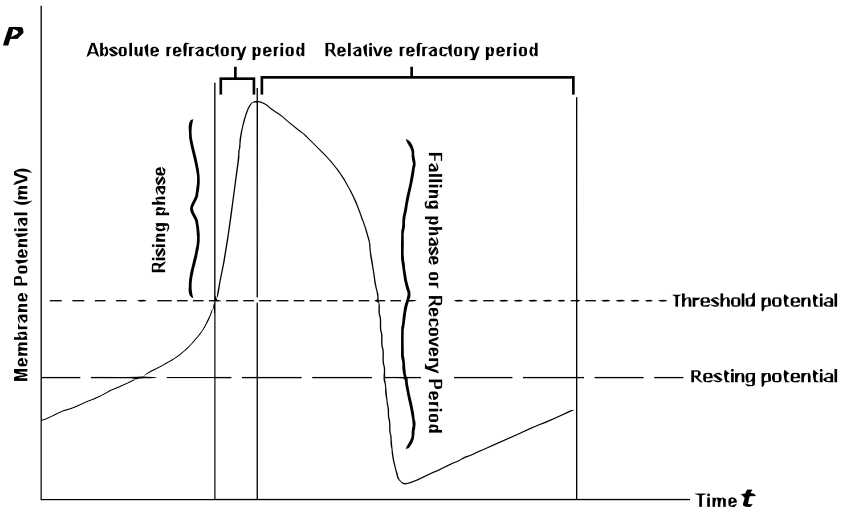

FIGURE 1. Neuron spike in the ($t$ime-Potential) plane obtained from experiments of neuron firing (see [12], [34] for details).

A more realistic model is one that depends on both space and time since electric currents cross the membrane of the cell and move along its axon lengthwise inside and outside. This mechanism makes it possible for electrical signals to be transmitted over long distance and thus propagate throughout the membrane without ever weakening or decreasing their initial strength. A mathematical model of the diffusion of current potential was first proposed and studied by FitzHugh in 1961, 1969 (see [12], [13]), Nagumo et al. in 1962 (see [28]) and many others.

Recent models have been proposed where the spatial solutions are conditioned by the effects of cross-diffusion "control" or "interactions" between components of the system ([27], [31], [25], [7], [5]).

Motivated by these works, we modified the FitzHugh model to include a cross-diffusion connection between the potential and recovery variables. We hypothesize that because of the semiconductor nature of the nerve membrane, the cross-diffusion regulation plays an important (perhaps crucial) role in the spatial spreading of potential ([29], [30], [37]). This version of the model will provide an avenue for investigating successful propagation of an excitable neuron but also propagation failures, which are extremely important for many applications (see, for example, [14], [15], [18] and Section 4 below). In this work we explore the changes of the characteristics of the spatial propagation of nerve impulses brought by changes in the velocity of propagation and intensity of the cross-diffusion regulation. In

particular, we are interested in the conditions of "normal" neuron firing propagation and investigate its possible violations. Some preliminary results were obtained in [3], [5].

The paper is organized in the following manner. Section 2 contains a brief description of local neuron dynamics within the framework of the FitzHugh model and the bifurcation portrait of the model. A cross-diffusion modification of the FitzHugh model aimed at providing an explanation of spatial modes like "traveling waves" is contained in Section 3. We show that fast and slow traveling waves can appear with respect to parameter values and follow their dependence with a bifurcation analysis of corresponding wave systems; we show also that the "traveling spike" appears only before some threshold value of the cross-diffusion coefficient. Section 4 contains the discussion of obtained results. Proofs of the statements of Section 3 are given in the Appendix.

2. **The FitzHugh equations as a local membrane model.** The original model of FitzHugh describing the dynamics of the physiological states of a nerve membrane contains the membrane potential variable, P, and the recovery variable, Q [12]. The variable P shares the properties of both the membrane potential and excitability and thus describes the dynamics of the *rising phase* of neuron firing. The variable Q is responsible for accommodation and refractoriness and thus represents the dynamics of the falling phase of the action potential. The equations are given by

$$\begin{aligned} P_\tau &= I - Q - P^3/3 + P, \\ Q_\tau &= \rho(a + P - bQ), \end{aligned} \tag{1}$$

where I is the stimulating current, ρ, a, and b are parameters of the system. FitzHugh in [12] and [13] described some types of qualitative dynamics of this system. The complete phase-parameter analysis of the FitzHugh model was given in [38]. With the change of variables and parameters

$$P \to P\sqrt{3}, Q \to Q\sqrt{3} + I, \tau = t/(\rho b), k_1 = 1/b, \varepsilon = \rho b, k_2 = (I - a/b)/\sqrt{3} \tag{2}$$

model (1) was reduced to the form[1]

$$\begin{aligned} \varepsilon P_t &= -P^3 + P - Q \equiv F_1(P, Q) \\ Q_t &= k_1 P - Q - k_2 \equiv F_2(P, Q), \end{aligned} \tag{3}$$

which contains only three parameters: $\varepsilon > 0$, $k_1 > 0$ and k_2. Volokitin and Treskov [38] investigated bifurcations of (3) depending on these parameters. Additionally, it was shown in [20] that the bifurcation of codimension 4 with symmetry, "3-multiple neutral singular point with the degeneration," is realized in the vector field defined by system (3) in a vicinity of the parameter point $\boldsymbol{M}$ ($k_1 = 1$, $k_2 = 0$, $\varepsilon = 1$). Some global stability results as well as the boundedness of solutions were proved in [23].

The system (3) has from one (a nonsaddle; i.e., a node or a spiral or center) up to three (two non-saddles and a saddle) singular points (P^*, Q^*) where P^* and Q^* are common roots of $F_1(P, Q)$ and $F_2(P, Q)$. A two-multiple singular point is a saddle or degenerate saddle. A three-multiple singular point $O(0, 0)$ arises at $k_1 = 1$, $k_2 = 0$; it is a degenerated spiral sink if $\varepsilon \neq 1$ [5]. The system can have also limit cycles. They can appear or disappear by three different ways: the Andronov-Hopf

[1] Volokitin and Treskov in [38] used the equivalent (for $b \neq 0$) change of variables: $P \to -P\sqrt{3}$, $Q \to Q\sqrt{3} - I$, $\tau = t/\varepsilon$, $k_1\varepsilon = \rho$, $bk_1 = 1$, $ak_1 = -(k_2\sqrt{3} + I)$.

subcritical bifurcation; the saddle-node bifurcation of limit cycles; the homoclinic bifurcation of a pair of separatrices of a saddle. In two former cases the cycle can contain a single singular point or three singular points. For the sake of brevity, we call a cycle "small" if it contains a unique singular point and "large" if it contains three singular points. The results presented in the following theorem were proven in [38].

Theorem 2.1. *(i) The space of parameters (k_1, k_2, ε) is subdivided into 21 domains of topologically different phase portraits of system (3). The cut of the complete (k_1, k_2, ε)-parameter portrait to the plane (k_1, k_2) is topologically equivalent to the diagram presented in Figures 2a, 3 for arbitrary fixed $0 < \varepsilon < 1$ and to the diagram presented in Figures 2b, 3 for arbitrary fixed $\varepsilon > 1$.*

The boundary surfaces in the parameter space correspond to the following bifurcations in system (3):

***S_1, S_2**: appearance/disappearance of a pair of singular points on the phase plane;*

***H_1^-, H_2^-**: change of stability of each of the nonsaddle singular points in the Andronov-Hopf subcritical bifurcation;*

***H_1^+, H_2^+**: change of stability of each of the nonsaddle singular points in the Andronov-Hopf supercritical bifurcation;*

***D**: appearance/disappearance of a pair of limit cycles;*

***P_1, P_2**: appearance/disappearance of a small limit cycle in one of two homoclinics of the saddle point;*

***R_1, R_2**: appearance/disappearance of a large limit cycle in one of two homoclinics of the saddle point.*

(ii) Boundaries corresponding to the local bifurcations of the singular points in the parametric space $\{k_1, k_2, \varepsilon\}$ are described by the following equations:

1) Surfaces

***S_1**: $k_2 = 2\sqrt{(1-k_1)^3/27}$, **$S_2$**: $k_2 = -2\sqrt{(1-k_1)^3/27}$, $0 \le k_1 \le 1$,*

***H_1**: $k_2 = (2 + \varepsilon - 3k_1)\sqrt{(1-\varepsilon)/27}$, $k_1 < \varepsilon \le 1$,*

***H_2**: $k_2 = -(2 + \varepsilon - 3k_1)\sqrt{(1-\varepsilon)/27}$, $k_1 < \varepsilon \le 1$;*

2) Lines

***SS**: $k_1 = 1, k_2 = 0$, **BT_1**, **BT_2**: $k_1 = \varepsilon$, $k_2 = \pm 2\sqrt{(1-\varepsilon)^3/27}, 0 < \varepsilon \le 1$,*

***DH_1**: $k_1 = 2 - \varepsilon$, $k_2 = 4(1-\varepsilon)\sqrt{(1-\varepsilon)/27}$,*

***DH_2**: $k_1 = 2 - \varepsilon$, $k_2 = -4(1-\varepsilon)\sqrt{(1-\varepsilon)/27}, 0 < \varepsilon \le 1$.*

Remark 1. The boundary surfaces in the parameter space (k_1, k_2, ε) correspond to the lines at the (k_1, k_2)-cut in Figure 2. Surfaces 1) correspond to bifurcations of codimension 1; lines 2) correspond to bifurcations of codimension 2. The curves of intersections of $\boldsymbol{S}_1$, $\boldsymbol{H}_2$ and $\boldsymbol{S}_2$, $\boldsymbol{H}_1$ as well as the curve of intersection of $\boldsymbol{H}_1^-$ and $\boldsymbol{H}_2^-$ correspond to bifurcations of codimension "1+1." The parameter and phase portraits possess certain symmetry: system (3) is symmetric under $(P, Q, k_1, k_2, \varepsilon) \to (-P, -Q, k_1, -k_2, \varepsilon)$; in particular, it is sufficient to study the systems for $k_2 \ge 0$. Because of this fact, certain phase portraits are given by number and index a, but the respective *symmetric* phase portraits have no number in the parameter portrait.

Let us emphasize that in the framework of the FitzHugh model the spike-regime (see Fig. 1) is the P-component of the trajectory $\{P(t), Q(t)\}$ corresponding to the large separatrix loop (which contains two singular points inside) in the phase plane. This loop is realized with parameter values $0 < k_1 < 1$, k_2, $0 < \varepsilon < 1$ belonging to the boundary $\boldsymbol{R}_1$ of the parameter portrait (see Fig. 2). The line $\boldsymbol{R}_1$

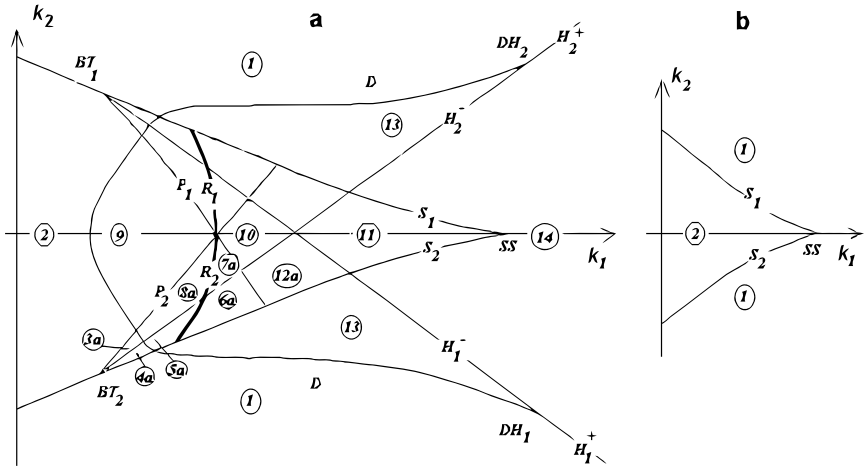

FIGURE 2. Schematic parameter portrait of FitzHugh model (3) and the fast wave systems (7+) of FitzHugh cross-diffusion model (for velocities $C^2 > Dk_1/\varepsilon$); **a** gives the ε-cut for $0 < \varepsilon < 1$, and **b** gives the ε-cut for $\varepsilon > 1$. Boundaries of domains: $\boldsymbol{S}_1$ and $\boldsymbol{S}_2$, saddle-node (fold) bifurcations in the phase plane; $\boldsymbol{H}_1^-$ and $\boldsymbol{H}_2^-$, the Andronov-Hopf subcritical bifurcations, $\boldsymbol{H}_1^+$ and $\boldsymbol{H}_2^+$, the Andronov-Hopf supercritical bifurcations; D, saddle-node limit cycle bifurcation; $\boldsymbol{P}_1$, $\boldsymbol{P}_2$, homoclinic bifurcations of the saddle point where separatrix loop contains a single non-saddle inside; $\boldsymbol{R}_1$, $\boldsymbol{R}_2$, homoclinic bifurcations of the saddle point where separatrix loop contains two non-saddles inside. See Theorems 2.1, 3.1(i) for the complete description of the boundaries of the domains. Boundary $\boldsymbol{R}_2$ corresponds to the neuron spike (Fig. 1). Refer to Figure 3 for the phase portraits in each domain.

adjacent domains 5a, 6a, 8a and 7a at the parametric portrait correspond to the most important regimes of our model. In domains 5a and 6a, system (3) is bistable: they have simultaneously a stable singular point and a stable large limit cycle (see Fig. 3). In domain 5a the basins of the stable regimes are divided by the unstable large limit cycle, which is its common boundary; in domain 6a the basins are more complex and are defined by the configuration of separatrices. In domains 7a and 8a system (3) is 3-stable: they have simultaneously two stable singular points and a stable large limit cycle (see Fig. 3). In domain 8a the basins of the large limit cycle and stable points are divided by the unstable large limit cycle (similarly to 5a); basins of stable singular points placed inside this limit cycle are divided by the unstable small limit cycle and the separatrices. Basins in domain 7a are more complex and also are defined by the configuration of separatrices (similarly to 6a) and by the unstable small limit cycle.

3. **Cross-diffusion model of a transmembrane potential.**

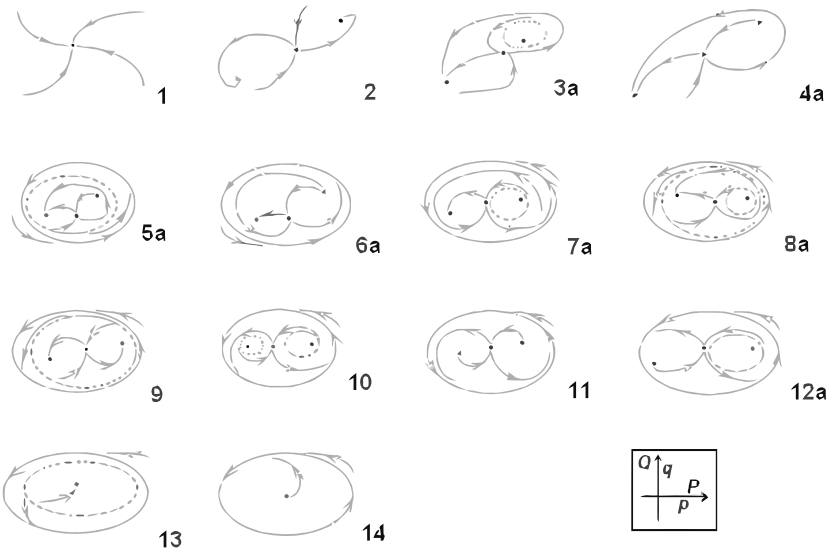

FIGURE 3. Schematic phase portraits corresponding to parameter domains from Fig. 2. The stable modes, periodic oscillations and equilibrium, are realized in domains 5a, 6a, 7a, 8a, 9, 10 adjacent to the boundary $\boldsymbol{R}_1$.

3.1. **Extending and modifying FitzHugh model.** In this section, we propose an extension of the FitzHugh spatial model to include the implicit (although hypothetical) cross-diffusion mechanism of the spatial propagation of the firing process of the neuron. The simplest version of the "space-distributed" FitzHugh - Nagumo model (FHN-model) for transmembrane potential accounts for the "current" $W_1(t,x)$ along the axon due to the gradient of the potential in the point x, so that $W_1(t,x) \sim -P_x$ (see [13], [28], [26, Ch. 6]). A more sophisticated approach may take into account another component of the current, $W_1(t,x) \sim -Q_x$, which defines the current against the gradient of the recovery variable. The total current $W(t,x)$ is then the sum of both components, and $P_t \sim -W_x$ (under zero local dynamics). Neglecting the possible currents of the recovery variable, we arrive at the model

$$\begin{aligned} \varepsilon P_t &= -P^3 + P - Q + DQ_{xx} + \sigma P_{xx}, \\ Q_t &= k_1 P - Q - k_2, \end{aligned} \tag{4}$$

where t is time, x is a one-dimensional space variable and nonnegative constants D, σ are the cross-diffusion and diffusion coefficients, respectively. The FHN-model corresponds to the "diffusion" version of system (4) with $D = 0, \sigma > 0$. Many works were devoted to the study of its dynamics, and in particular, to the investigation of "traveling wave" solutions ([17], [11], [32], [9], [33]). A bifurcation approach applied to the study of traveling impulses and trains (see [24]) revealed that "fast" and "slow" waves can exist with the same values of "local parameters" ε, k_1.

To clarify the role of the spatial distribution of the recovery variable (along the axon) and the meaning of the cross-diffusion term in the impulse propagation, we consider a cross-diffusion version of system (4):

$$\begin{aligned} \varepsilon P_t = -P^3 + P - Q + DQ_{xx} &\equiv F_1(P,Q) + DQ_{xx} \\ Q_t = k_1 P - Q - k_2 &\equiv F_2(P,Q). \end{aligned} \tag{5}$$

Mathematically, cross-diffusion equations possess special properties, which facilitate their research [40], [3], [5].

3.2. **Wave system of the model.** In what follows, we explore "traveling wave" solutions of system (5):

$$P(x,t) = P(x+Ct) \equiv p(\xi),\ Q(x,t) = Q(x+Ct) \equiv q(\xi),$$

where $\xi = x + Ct$ and positive C is the velocity of the wave propagation. It can be checked that $(p(\xi), q(\xi))$ satisfy the following *two-dimensional* "*wave system*":

$$\begin{aligned} (\varepsilon C^2 - Dk_1)/C p_\xi &= F_1(p,q) - DF_2(p,q)/C^2, \\ C q_\xi &= F_2(p,q). \end{aligned} \tag{6}$$

Thus, the problem of describing all traveling wave solutions of system (5) and their rearrangements is reduced to the analysis of phase curves and bifurcations of solutions of wave system (6), which has the additional parameter C.

Let us denote $\alpha = C^2/(\varepsilon C^2 - Dk_1)$ and $\beta = \mathrm{sign}(\alpha)$. As we show further, the behavior of the wave system essentially depends on the sign of the parameter α and thus we distinguish the cases $\beta =$"+" and $\beta =$"−." We change the independent variable $\eta = \xi/C$ and then wave system (6) becomes

$$p_\eta = \alpha(F_1(p,q) - DF_2(p,q)/C^2), \tag{7β}$$

$$q_\eta = F_2(p,q),$$

where $F_1(p,q) = -p^3 + p - q, F_2(p,q) = k_1 p - q - k_2$. This system is defined at $\varepsilon C^2 \neq Dk_1$.

We show that systems (7+) with $C > \sqrt{Dk_1\varepsilon}$ and (7−) with $C < \sqrt{Dk_1\varepsilon}$ demonstrate qualitatively different behaviors under variations of "local" parameters ε, k_1, k_2. In other words, the parabola $C^2 = Dk_1/\varepsilon$ is the boundary between domains of qualitatively different behaviors of wave system (6) in the (D, C)-parameter plane under fixed values of "local" parameters ε, k_1, k_2. In what follows we will omit the symbol β in (7β) when we study the system properties that do not depend on β.

3.3. **Phase-parametric portraits of the wave systems.** System (7+) with $C^2 > Dk_1/\varepsilon$ is called the *fast* wave system, whereas system (7−) with $C^2 < Dk_1/\varepsilon$ is called the *slow* wave system of model (5). For both cases system (7β) evidently has from one up to three singular points (p^*,q^*) where p^* and q^* are common roots of $F_1(p,q)$ and $F_2(p,q)$. Two singular points coincide and form a 2-multiple point with the parameter values belonging to boundaries $\boldsymbol{S}_1$ and $\boldsymbol{S}_2$ (see Fig. 2 and Theorem 2.1). Thus, both the fast and slow wave systems have three singularities inside the curvilinear angle that is formed by $\boldsymbol{S}_1$ and $\boldsymbol{S}_2$, and a single singular point outside the angle. Note that this unique singular point is a nonsaddle (a node or spiral) for the fast wave system whereas it is a saddle for the slow one. Inside the parameter angle the fast wave system has two nonsaddles and a saddle, whereas the slow one has two saddles and one nonsaddle (see Proposition 3 in the Appendix).

At $k_1 = 1, k_2 = 0$ the points coincide in a 3-multiple singular point $O(0,0)$ which is a nonhyperbolic spiral if $\varepsilon \neq 1$ for the fast wave system and a nonhyperbolic saddle for the slow wave system.

Theorem 3.1. *(i) Let $C^2 > Dk_1/\varepsilon$. For any positive fixed α there exists a neighborhood $\Omega = \Omega(\alpha)$ of the parameter point $(k_1 = 1, k_2 = 0, \varepsilon = 1)$ in which the space of parameters (k_1, k_2, ε) of system (7+) is subdivided into 21 domains of topologically different phase portraits. The cut of complete (k_1, k_2, ε)-parameter portrait to the plane (k_1, k_2) is topologically equivalent to the diagrams presented in Figures 2a and 3 for arbitrary fixed $0 < \varepsilon < 1$ and to the diagram presented in Figures 2b and 3 for arbitrary fixed $\varepsilon > 1$.*

The boundary surfaces in the parameter space correspond to the following bifurcations in system (7+):

S$_1$, ***S***$_2$*: appearance/disappearance of a pair of singular points in the phase plane;*

H$_1^-$, ***H***$_2^-$*: change of stability of each of the non-saddle singular points in the Andronov-Hopf subcritical bifurcation;*

H$_1^+$, ***H***$_2^+$*: change of stability of each of the non-saddle singular points in the Andronov-Hopf supercritical bifurcation;*

D*: appearance/disappearance of a pair of limit cycles;*

P$_1$, ***P***$_2$*: appearance/disappearance of a small limit cycle in one of two homoclinics of the saddle point;*

R$_1$, ***R***$_2$*: appearance/disappearance of a large limit cycle in one of two homoclinics of the saddle point.*

(ii) Let $C^2 < Dk_1/\varepsilon$. For any negative fixed α there exists a neighborhood $\Omega = \Omega(\alpha)$ of the parameter point $(k_1 = 1, k_2 = 0, \varepsilon = 1)$ in which the space of parameters (k_1, k_2, ε) of system (7−) is subdivided into 10 domains of topologically different phase portraits. The cut of complete (k_1, k_2, ε)-parameter portrait to the plane (k_1, k_2) is topologically equivalent to the diagram presented in Figures 4a and 5 for arbitrary fixed positive $0 < \varepsilon < 1$ and in Figures 4b and 5 for arbitrary fixed $\varepsilon > 1$.

The boundary surfaces in the parameter space correspond to the following bifurcations:

S$_1$, ***S***$_2$*: appearance/disappearance of a pair of singular points in the phase plane;*

H$^-$*: change of stability of the unique non-saddle singular point in the Andronov-Hopf subcritical bifurcation;*

P^1, ***P***^{2}*: appearance/disappearance of a small limit cycle in homoclinics of each of the saddle points;*

L^1, ***L***^{2}*: upper and lower (respectively) heteroclinics of saddle points.*

The proofs of Theorems 2.1 and 3.1 are given in the Appendix.

Remark 2. For fixed values of α system (7β) is symmetric under $(p, q, k_1, k_2, \varepsilon) \to (-p, -q, k_1, -k_2, \varepsilon)$. In particular it is sufficient to study the systems for $k_2 \geq 0$. Due to this fact, we present in the schematic bifurcation diagram only certain parameter and phase portraits. The portraits, which are symmetric, are given by number and index a, see Figures 2a, 2b, and 3 for system (7+) and Figures 4a, 4b, and 5 for system (7−).

3.4. **Traveling wave solutions of PDE and their profiles as solutions of wave ODE.** The correspondence between traveling wave solutions of PDE model and orbits of its wave system is well known (see [39], [4], [5]) and schematically is

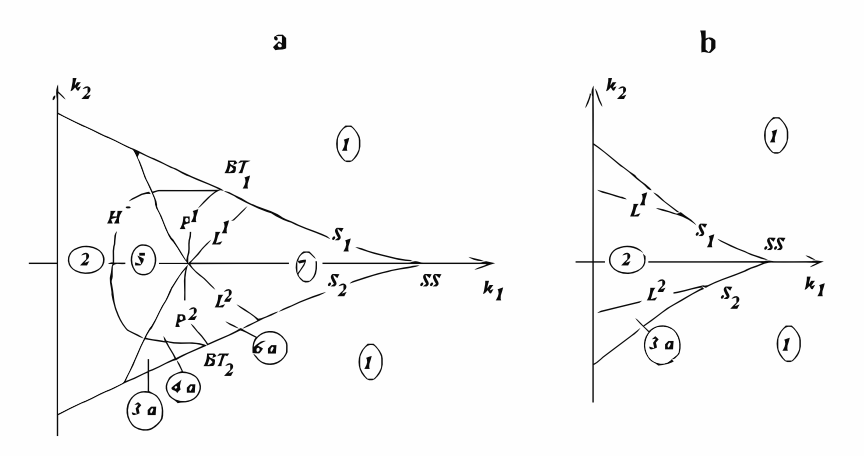

FIGURE 4. Schematic parameter portrait of the slow wave systems (7-) of FitzHugh cross-diffusion model (for velocities $C^2 < Dk_1/\varepsilon$); **a** gives the ε-cut for $0 < \varepsilon < 1$, and **b** gives the ε-cut for $\varepsilon > 1$. Boundaries of domains: $\boldsymbol{S}_1$ and $\boldsymbol{S}_2$, saddle-node (fold) bifurcations in the phase plane; $\boldsymbol{H}^-$, the subcritical Andronov-Hopf bifurcations; $\boldsymbol{P}^1$, $\boldsymbol{P}^2$, homoclinic bifurcations of the saddle point where separatrix loop contains a single non-saddle inside; $\boldsymbol{L}^1$, $\boldsymbol{L}^2$, heteroclinics of saddle singular points. See Theorem 3.1(ii) for the complete description of the boundaries of the domains. Refer to Figure 5 for the phase portraits in each domain.

given in Figures 6–8. We make this correspondence more formal with the following statement.

Proposition 1. *i) A spatially homogeneous solution of the model corresponds to a singular point of the vector field defined by the wave system;*

ii) a wave front of the model corresponds to a heteroclinic curve of the wave system which joins singular points (which are saddles) with different p-coordinates, see Figure 6a, b;

iii) a wave impulse of the model corresponds to a homoclinic curve (separatrix loop) of a singular point of the wave system (see Figure 7 where the small loops in (a) and (b), containing one singular point inside, and the large loop in (c), containing two singular points, are shown);

iv) a wave train of the model corresponds to a limit cycle in the (p, q) phase plane of the wave system, see Figure 8.

3.5. **Fast and slow traveling waves of the cross-diffusion system.** Applying Proposition 1, Theorem 3.1, and using the bifurcation diagrams of systems (7+) and (7−), we can now prove the following theorems, which completely describe the fast and slow traveling wave solutions of model (5).

Theorem 3.2. *Model (5) has the fast traveling wave solutions (i.e., with $C^2 > Dk_1/\varepsilon$) of the following types:*

(a) the fronts in every domain of the portraits shown in Figure 2, except domains 1, 13, 14, see Figure 6;

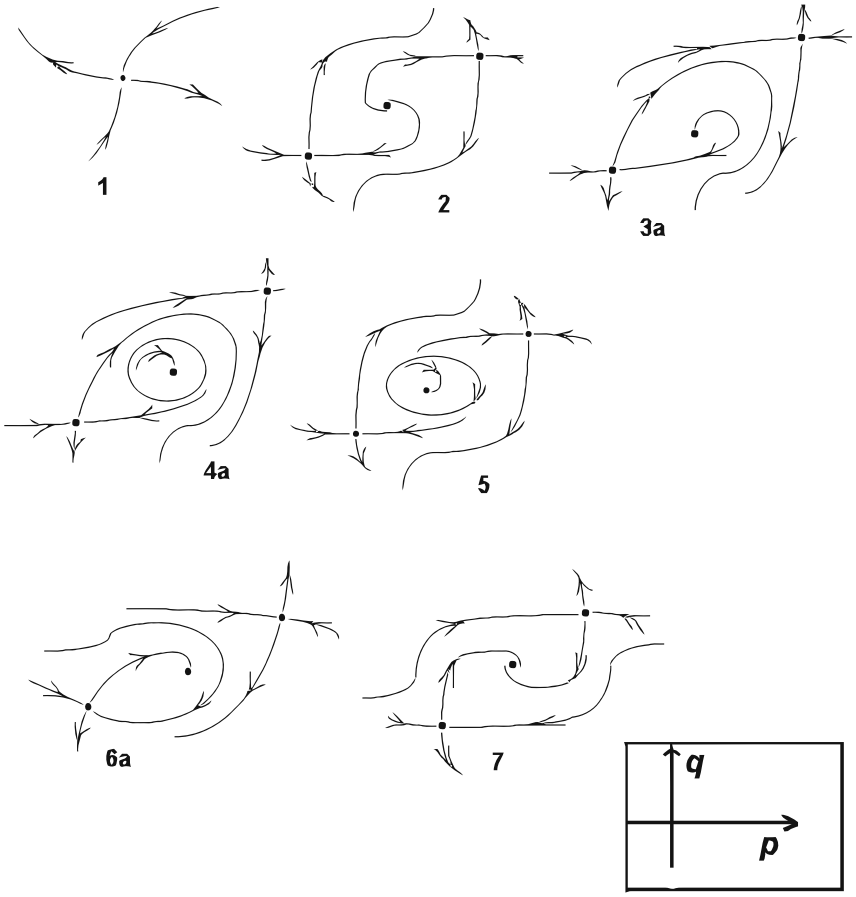

FIGURE 5. Schematic phase portraits corresponding to parameter domains from Figure 4.

(b) the single train in domains 3a,b, 6a,b, 11, 14; two trains, differing in their "amplitudes", in domains 5a,b, 7a,b, 9, 12a,b, 13; three different trains in domains 10 and 8a,b (see Fig. 2a and Fig. 8);

(c) the impulses on the boundaries $\boldsymbol{P}_1$, $\boldsymbol{P}_2$ *and* $\boldsymbol{R}_1$, $\boldsymbol{R}_2$, *see Figure 2a and Figure 7a,b,c.*

Theorem 3.3. *Model (5) has the slow traveling wave solutions (i.e., with* $C^2 < Dk_1/\varepsilon$*) of the following types:*

(a) the fronts in every domain of the portrait in Figure 4a and 4b except the domain 1; monotonous fronts with the maximal "amplitude" on the boundaries $\boldsymbol{L}^1$, $\boldsymbol{L}^2$ *(see Fig. 6);*

(b) the trains in the domains 4a,b, 5 of the portrait in Figure 4a (see Fig. 8);

(c) the impulses on the boundaries $\boldsymbol{P}^1$, $\boldsymbol{P}^2$ *of the portrait in Figure 4a (see Fig. 7a,b).*

4. **Discussion and conclusion.**

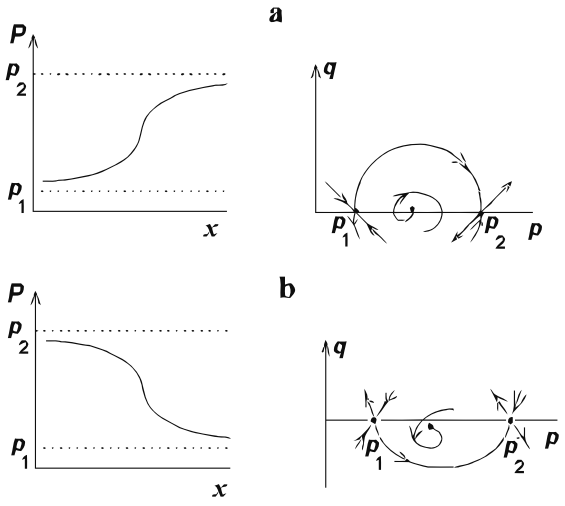

FIGURE 6. Wave front solutions of PDE (5) satisfy boundary conditions: $P(x) \to p_2$ for $x \to \infty$ and $P(x) \to p_1$ for $x \to -\infty$; the solutions correspond to monotonous *heteroclinic curves* in the (p, q)-plane of the ODE wave system (7).

4.1. **Scenarios of appearance and transformations of the traveling waves.** The problem of our interest is the appearance and transformations of the traveling wave solutions depending on the model parameters D and C that characterize the axon abilities for the firing propagation. (One could assume that these characteristics may change as a result of influence of certain drugs or external chemicals.) The bifurcation diagram shown in Figures 4 and 5 corresponds to the wave system of FH-model (5) with "large" $D > \varepsilon C^2/k_1$. The bifurcation diagram shown in Figures 2 and 3 corresponds to the wave system of model (5) with a "small" cross-diffusion coefficient $0 \le D < \varepsilon C^2/k_1$ (and that this diagram coincides with the bifurcation diagram of the local Fitz-Hugh model (3)). Thus, these diagrams describe the model behavior *before* and *after* the threshold $D = \varepsilon C^2/k_1$ accordingly, where C is the fixed propagation speed.

We now trace the transformation of the traveling wave solutions by varying the parameters C and D under the supposition that parameters k_1, k_2, ε have arbitrary fixed values close to the point $k^*{}_1 = 1, k^*{}_2 = 0, \varepsilon^* = 1$. The parametric point $(k^*{}_1, k^*{}_2, \varepsilon^*)$ is the *organizing center* of the model, because all the main behaviors of the model are realized in a neighborhood of this point [20]. Let the (positive) value of the speed propagation C be fixed and suppose the cross-diffusion coefficient increases. For $D = 0$ the wave system of the model coincides with the local FitzHugh model. This model demonstrates a spike (shown in Fig. 1) if (k_1, k_2, ε) belongs to the boundary $\boldsymbol{R}_2$. The wave system describes "pseudowaves" and, in reality, there is no firing propagation.

Let $D > 0$. Due to Theorems 3.2 and 3.3 the model at $D < C^2\varepsilon/k_1$ and $(k_1, k_2, \varepsilon) \in \boldsymbol{R}_2$ has a traveling spike spreading along the axon with velocity C. This spike has a "large" propagation velocity, $C > \sqrt{Dk_1/\varepsilon}$, and "large" amplitude. More exactly, the p-amplitude of the spike $\{p(\xi), q(\xi)\}$ is greater than $|p_3 - p_1|$,

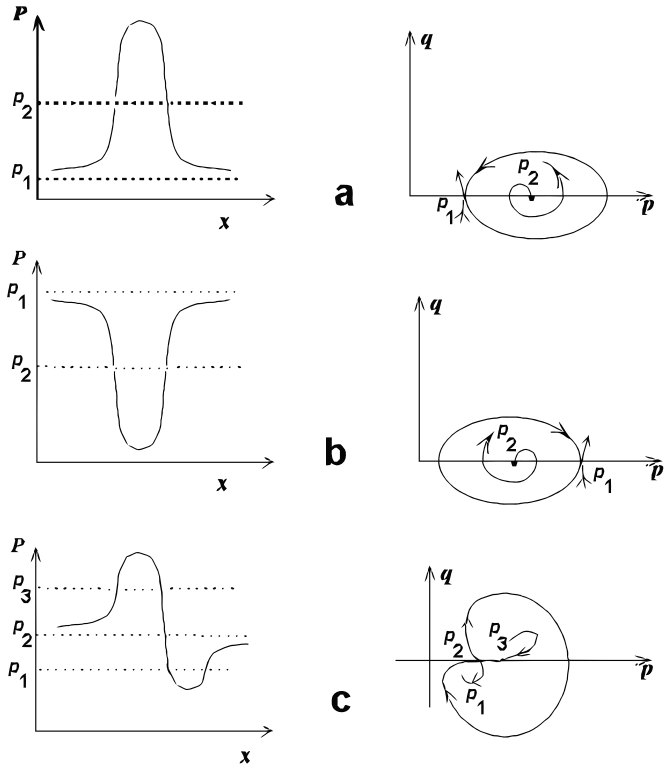

FIGURE 7. Wave-impulses of PDE (5) satisfy boundary conditions: $P(x) \to p_1$ for $x \to \pm\infty$ or $P(x) \to p_2$ for $x \to \pm\infty$; they correspond to *homoclinic curves* in the (p, q)-plane of the ODE wave system. Three typical pictures are given in figures **a**, **b**, and **c**.

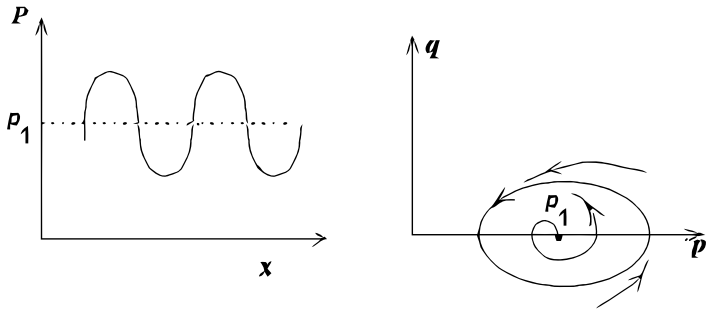

FIGURE 8. Wave-train solutions of PDE (5) correspond to *limit cycles* in the (p, q)-plane of the ODE wave system.

where $p_1 < p_2 < p_3$ are the roots of the polynomial $F_1(p, k_1p - k_2) = -p^3 + p(1 - k_1) + k_2$.

Let us note that as $C \to \infty$ parameter $\alpha(C) \to 1/\varepsilon$; hence the wave system (7) formally becomes the local system (3). The bifurcation diagram given in Figures 2 and 3 allows us to identify all other possible waves, namely, trains with "large" and "small" p-amplitude (the latter if it is less than either $|p_2 - p_1|$ or $|p_3 - p_2|$) and fronts with nonmonotonic tails.

On the contrary, if $D > \varepsilon C^2/k_1$, then a traveling spike does not exist. The only possible traveling waves are "small" trains, impulses or fronts with the p-amplitudes less than $|p_3 - p_1|$. The velocity C of propagation of these waves is less than $\sqrt{Dk_1/\varepsilon}$. The bifurcation diagram given in Figures 4 and 5 allows us to describe transformations of waves with the changing of their velocity. If a parametric point (k_1, k_2, ε) belongs to domain 6a, then the sole traveling wave solution $\{p(\xi), q(\xi)\}$ is the wave-front with nonmonotonic tail. When the velocity C increases (under the condition $C < \sqrt{Dk_1/\varepsilon}$), the system intersects the boundary $\boldsymbol{L}^1$ and enters into domain 7. There exist two slow wave-fronts with nonmonotonic tails moving with the same velocity from the right to the left; their p-amplitudes are $|p_2 - p_1|$ and $|p_3 - p_2|$, correspondingly. When C increases, both waves become monotonic; for $C = \sqrt{Dk_1/\varepsilon}$ the first equation of wave system (7$-$) is degenerate and describes the curve $q = -p^3 + p(1 - k_1) + k_2$ that smoothly joins the points p_1, p_2, p_3. Further increase of C leads to a "transformation" of the slow wave system into the fast one, and thus to the appearance of waves similar to the spike spreading along an axon. A behavior of the model under critical values $D = C^2\varepsilon/k_1$, evidently, cannot be studied in the framework of the two-dimensional model (5).

4.2. **Possible role of cross-diffusion mechanism.** We utilized a modified version of the FitzHugh equations to model the spatial propagation of neuron firing; we assumed that this propagation is essentially caused by the cross-diffusion connection between the potential and recovery variables. This modification, which includes the implicit (although hypothetical) cross-diffusion mechanism, could help explore the effect of a generic drug in the neuron firing process.

For example, the influence of certain drugs or external chemicals affects the rate at which sodium channels close and the rate at which potassium channels open, thus altering the normal dynamics of a firing potential membrane. A study conducted by [14], [34] showed that certain metabolites in ethanol accelerate the release of potassium ions from the brain cells. The increased potassium efflux in turn makes it difficult for cells to absorb enough calcium and thus inhibits the release of neurotransmitters [18]. The changes in the release of potassium ions result in the changes in the recovery phase of the excitable membrane. In addition, at any given time "there are circulating currents that cross the membrane and flow lengthwise inside and outside the axon and the membrane current and potential vary with distance as well as with time" [12]. A generic drug that alters the flow of potassium has an effect on the neuron returning to its rest potential and may change characteristics of axon conductivity that accelerate or delay a spatial propagation of a firing potential. We include this effect of a generic drug by incorporating a cross-diffusion term in the original FitzHugh model.

The mathematical problem of our interest was the appearance and transformations of the traveling wave solutions, which depended on the model parameters D (the cross-diffusion coefficient) and C (the propagation speed) that characterize

the axons abilities for the firing propagation. We studied the wave system of the cross-diffusion version of the model and explored its bifurcation diagram.

We have shown that the cross-diffusion model possesses a large set of traveling wave solutions; besides giving rise to the typical "fast" traveling wave solution exhibited in the original "diffusion" FitzHugh-Nagumo equations, it also gives rise to a "slow" traveling wave solution. This more sophisticated approach indicates that instead of a "one-parametric" set of waves ordered by the propagation speed C, one should consider a two-parametric set of traveling wave solutions with parameters (C, D). We then proved that in the parametric space (D, C) (under fixed parameter values ε, k_1, k_2) there exists a parabolic boundary, $D = KC^2$, where constant $K = \varepsilon/k_1$, which separates the domains of existence of the fast and slow waves. The system behavior qualitatively changes with the intersection of this boundary. Let us emphasize that the "traveling spike" that we consider as the "normal" propagation of a nerve impulse is a "fast" traveling wave. Hence, the parabola $D = KC^2$ bounds the area where the "normal" spike propagation is possible. After the intersection of this boundary, due to a very large cross-diffusion coefficient or too small speed of impulse propagation, a "normal" propagation of the nerve impulse is impossible and some violations are inevitable: nerve impulses propagate with decreasing amplitude or as damping oscillations.

The cross-diffusion regulations in the FitzHugh model allowed us to observe the propagation of spikes and spike-like oscillations but restricted their velocities from below or, equivalently, maintained the upper boundary for the cross-diffusion coefficient. It means that if, by any reasons (e.g., as a result of the effect of a generic drug) the speed of transmission of a signal along the axon is reduced, then the "normal" neuron firing propagation in the form of a traveling spike is impossible. The increase of the cross-diffusion coefficient beyond the "normal" value implies the same result.

5. **Mathematical Appendix. Proof of Theorem 3.1.**

5.1. **Lienard form of the wave system.** By the change of variables $(P, Q) \to (U, Z)$:

$$U = Q + k_2, Z = F_2(P, Q) \equiv k_1 P - Q - k_2, \tag{8}$$

the local model (3) is transformed to the generalized Lienard form:

$$\begin{aligned} U_t &= Z, \\ \varepsilon Z_t &= f(U) + Z(g_1(U) + ZG(U, Z)) \equiv \Phi(U, Z), \end{aligned} \tag{9}$$

where

$$\begin{aligned} f(u) &= -u^3/k_1^2 + u(1 - k_1) + k_1 k_2 \\ g_1(u) &= (1 - \varepsilon) - 3u^2/k_1^2 \\ G(u, z) &= -(3u + z)/k_1^2. \end{aligned} \tag{10}$$

Note, that model (5) after transformation (8) reads as the cross-diffusion modification of (9) with the coefficient Dk_1:

$$\begin{aligned} U_t &= Z, \\ \varepsilon Z_t &= \Phi(U, Z) + Dk_1 U_{xx}, \end{aligned} \tag{11}$$

A *traveling wave solution* of system (11) is defined as a pair of bounded functions

$$U(x,t) = u(x+Ct) \equiv u(\xi),\ Z(x,t) = z(x+Ct) \equiv z(\xi)$$

where $C > 0$ is a velocity of propagation. After introducing an independent variable $\eta = \xi/C$ the functions $\{u(\eta), z(\eta)\}$ satisfy the *wave system*

$$u_\eta = z,\ z_\eta = \alpha\Phi(u,z) \equiv F(u,z;\alpha). \tag{12β}$$

Here $\alpha = C^2/(\varepsilon C^2 - Dk_1)$ if $C^2 \neq Dk_1/\varepsilon$, $\beta = \mathrm{sign}(\alpha)$ and $F(u,z;\alpha) = \alpha f(u) + \alpha z g_1(u) + \alpha z^2 G(u,z)$ with $f(u), g_1(u)$ and $G(u,z)$ given by (10). Note, that $\alpha = 1/\varepsilon$ if $D = 0$ and $\varepsilon \neq 0$; it means that the vector field defined by system (12+) coincides with the vector field defined by system (9).

Let's now replace the capital letters in (8) by small letters, reduce p and q via

$$p = (z+u)/k_1,\ q = u - k_2\ (k_1 \neq 0),$$

and substitute into system (7β). Dividing the equation for u_ξ by $C \neq 0$ we get system (12β).

In what follows we consider system (12β) instead (7β).

5.2. **Main characteristics of the vector fields depending on α.** Consider the generalized Lienard vector field:

$$\boldsymbol{J} = z\partial/\partial u + F(u,z;\alpha)\partial/\partial z \tag{13}$$

where

$$\begin{aligned} F(u,z;\alpha) &= \alpha(f(u) + z(g_1(u) + zG(u,z))), \\ f(u) &= -au^3 + u\delta_1 + \delta_2, \\ g_1(u) &= \delta_3 - 3au^2, \\ G(u,z) &= -a(3u+z) \end{aligned} \tag{14}$$

with positive constant a, arbitrary $\alpha \neq 0$ and "small" parameters $\delta_1, \delta_2, \delta_3$.

Proposition 2. *Let $\delta_1 = 1 - k_1$, $\delta_2 = k_2k_1$, $\delta_3 = 1 - \varepsilon$, $a = 1/k_1^2$ and $\alpha^* = C^2/(\varepsilon C^2 - Dk_1)$. Then vector field (13)-(14) coincides with vector field given by system (9) if $\alpha = 1/\varepsilon$ and with vector field given by system (12β) if $\alpha = \alpha^*$.*

For any α, $0 < \alpha < \infty$ vector field (13)-(14) has at least one singular point $(u_0, 0)$ where u_0 is a root of the cubic polynomial $f(u) = -au^3 + u\delta_1 + \delta_2$.

Proposition 3. *For positive α vector field (13)-(14) has a single (non-saddle) singular point outside the curvilinear angle formed by curves $\delta_2 = \pm 2(\delta_1^3/27a)^{1/2}$ and three (two nonsaddles and one saddle) singular points inside this angle; for negative α vector field (13)-(14) has a single (saddle) or three (two saddles and one nonsaddle) singular points outside and inside, respectively, the curvilinear angle.*

Proof. The Jacobian of (13)-(14) at point $(u_0, 0)$ is:

$$A(\boldsymbol{J}) = \begin{pmatrix} 0 & 1 \\ f_u(u_0) & g_1(u_0) \end{pmatrix}.$$

For $\delta_1 = 0$ the vector field has the unique singularity $(u_0, 0) = ((\delta_2/a)^{1/3}, 0)$. The Jacobian determinant at $(u_0, 0)$, $\det(A) = 3\alpha u_0^2$, is positive for positive α, so the singular point is a nonsaddle and negative for negative α, so the point is a saddle

[1], [16]. Because of standard continuity arguments, for small δ_1 the polynomial $f(u)$ has a root u_0^* close to u_0, $\det(A)$ preserves its sign and the type of singular point remains unchanged.

For arbitrary $\delta_1 \neq 0$, $f(u)$ may have two additional roots. An appearance of these roots corresponds to the appearance of two additional singular points of the vector field. Generally, these additional points are a saddle and a node (see, for example, [16], [23]). They are seen to come into existence when

$$-au^3 + u\delta_1 + \delta_2 = 0,\ -3au^2 + \delta_1 = 0,$$

and one can easily find the boundaries of the *curvilinear angle* in (δ_1, δ_2)-space that correspond to existence of two-multiple roots u_0 of polynomial $f(u)$. □

5.3. **Main part of vector field (13).**

(A) Generalized Lienard vector field (13) with $F(u, z; \alpha) = h(u) + zr(u) + z^2\varphi(z, u)$, where $h(u), r(u), \varphi(z, u)$ are polynomials, $\varphi(0, 0) = 0$, can be reduced by non-degenerate change of variables $(z, u) \to (y_1, y_2)$ to the Lienard vector field (13) where

$$F(y_1, y_2; \alpha) = h(y_1) + y_2 r(y_1) \tag{15}$$

(see [2]).

(B) Vector field (13), (15) with $h(y_1) = \mu_2 + \mu_1 y_1 + \gamma y_1^3 + O(y_1^4)$, $r(y_1) = (\mu_3 + \mu_4 y_1 + \nu y_1^2 + O(y_1^3))$ where $\gamma\nu \neq 0$ is C^∞-equivalent to vector field (13) with $h(y_1) = \mu_2 + \mu_1 y_1 + \gamma y_1^3$ and $r(y_1) = \mu_3 + \mu_4 y_1 + \nu y_1^2$ where $\nu = \pm 1$ and $\gamma = \pm 1$; the bifurcation diagrams for $\gamma = 1$ and $\gamma = -1$ are topologically nonequivalent ([35], [10]); the complete unfolding for $\mu_4 \neq 0$ was presented in the latter work.

Because of assertions (A), (B) for small $\delta_1, \delta_2, \delta_3$ unfolding of vector field (13), (14) coincides with the unfolding of vector field

$$\overline{\boldsymbol{J}} = z\partial/\partial u + P(u, z; \alpha)\partial/\partial z \tag{16}$$

where

$$P(u, z; \alpha) = \alpha(f(u) + zg_1(u)), f(u) = -au^3 + u\delta_1 + \delta_2, g_1(u) = \delta_3 - 3au^2. \tag{17}$$

System

$$u_\eta = z,\ z_\eta = P(u, z; \alpha) \tag{18β}$$

corresponds to $\overline{\boldsymbol{J}}$.

(C) For fixed values α and a system (18β) is symmetric under $(z, u, \delta_1, \delta_2, \delta_3) \to (-z, -u, \delta_1, -\delta_2, \delta_3)$. In particular, it is sufficient to study the systems for $\delta_2 \geq 0$.

5.4. **Proof of Theorem 3.1(i).** Here we study the case $\alpha > 0$ in system (12β). We need the following theorem ([20]).

Theorem 5.1 (Khibnik, Krauskopf, Rousseau, 1998)**.** *(1) There exists a neighborhood of the parametric point $(\mu_1, \mu_2, \mu_3) = (0, 0, 0)$ in which any system of the form*

$$y_1' = y_2,\ y_2' = h(y_1) + y_2 r(y_1) \tag{19}$$

where $h(y_1) = \mu_2 + \mu_1 y_1 - y_1^3, r(y_1) = (\mu_3 - y_1^2)$, has a bifurcation diagram in a neighborhood of the phase point $(y_1 = 0, y_2 = 0)$, whose cut to the plane (μ_1, μ_2) for arbitrary $\mu_3 > 0$ and $\mu_3 < 0$ is topologically equivalent to the diagrams presented in Figures 2a, 3 and Figures 2b, 3.

(2) The boundaries in the parameter portrait given in Figure 2 corresponding to the local bifurcations of codimension 1 are the surfaces

S: *saddle-node bifurcation, given by* $4\mu_1^3 - 27\mu_2^2 = 0$ *and*

H: *Andronov-Hopf bifurcation, given by* $\mu_3^3 - 2\mu_3^2\mu_1 + \mu_3\mu_1^2 - \mu_2^2 = 0$ *for* $\mu_3 \geq \frac{\mu_1}{3}$.

(3) The boundaries in the parameter portrait corresponding to the local bifurcations of codimension 2 are the curves

SS: *cusp bifurcation, given by* $\mu_1 = \mu_2 = 0, \mu_3 \neq 0$*;*

BT: *Bogdanov-Takens bifurcation, given by the system* $4\mu_1^3 - 27\mu_2^2 = 0$, $\mu_1 - 3\mu_3 = 0$*; and*

DH: *degenerate Andronov-Hopf bifurcation of order two, given by the system* $\mu_1 + 3\mu_3 = 0$, $16\mu_3^3 - \mu_2^2 = 0$, *and in any perturbation the outmost limit cycle is stable. For* $\mu_1 + 3\mu_3 < 0$ *the Andronov-Hopf bifurcation is supercritical and for* $\mu_1 + 3\mu_3 > 0$ *it is subcritical.*

(4) The boundaries in the parameter portrait given in Figure 2 corresponding to the non-local bifurcations of codimension 1 are the surfaces

D: *double limit cycles;*

$\boldsymbol{P_1}$**,** $\boldsymbol{P_2}$**:** *homoclinics of the saddle containing one non-saddle inside itself; and*

$\boldsymbol{R_1}$**,** $\boldsymbol{R_2}$**:** *homoclinics of the saddle containing two non-saddles inside itself.*

Let us reduce system (18β) to the form (19). For any $\alpha > 0$ we use scaling

$$u = Ay_1, z = By_2, \eta = 3\tau \tag{20}$$

with

$$A = \frac{1}{3a^{1/2}\alpha^{1/2}}, B = \frac{1}{9a^{1/2}\alpha^{1/2}}, a = 1/k_1^2. \tag{21}$$

Then

$$\mu_1 = 9\alpha\delta_1, \mu_2 = 27a^{1/2}\alpha^{3/2}\delta_2, \mu_3 = 3\alpha\delta_3. \tag{22}$$

Evidently, μ_1, μ_2, μ_3 are small parameters if $k_1 \approx 1, k_2 \approx 0, \varepsilon \approx 1$, i.e., if $\delta_1, \delta_2, \delta_3$ are small, and the main assertions of Theorem 3.1 (i) for parameter point $(k_1, k_2, \varepsilon) = (1, 0, 1)$ follows from parts (1)-(3) of Theorem KKR.

Next, the divergence $\operatorname{div}\widehat{J}$ of vector field (19) is negative, $\operatorname{div}\widehat{J} = r(y_1) = (\mu_3 - y_1^2) < 0$ for $\mu_3 < 0$. Hence, vector field (16)-(17) with $\alpha > 0$ has no closed orbits and separatrix loops for any $\delta_3 < 0$ because $\mu_3 = 3\alpha\delta_3$. Applying Proposition 2 and assertions (A) and (B) we can state that the ε-cuts of the parameter portrait of vector field (7+) coincides with those given in Figures 2a and 2b. Statement (i) of Theorem 3.1 is completely proved.

Corollary 1. *For vector field (13)-(14) with* $\alpha > 0$ *the boundaries of the parameter portrait corresponding to the fold, cusp and Bogdanov-Takens bifurcations are given by the equations, respectively,*

$$\begin{aligned} \boldsymbol{S}: &\quad \{27a\delta_2^2 = 4\delta_1^3, a \neq 0\}; \\ \boldsymbol{SS}: &\quad \{\delta_1 = \delta_2 = 0, a \neq 0\}; \\ \boldsymbol{BT}: &\quad \{\delta_1 = \delta_3, 27a\delta_2^2 = 4\delta_3^3, a \neq 0\}. \end{aligned} \tag{23}$$

The boundaries corresponding to the subcritical ($\boldsymbol{H}^-$*), supercritical (*$\boldsymbol{H}^+$*) and degenerate Andronov-Hopf bifurcations are given by the equations, respectively,*

$$\begin{aligned} \boldsymbol{H}^{-}: &\quad \{\delta_3(-3\delta_1+\delta_3)^2 = 27a\delta_2^2, \delta_3>0, \delta_1<\delta_3, -\delta_1<\delta_3, a\neq 0\}, \quad (24)\\ \boldsymbol{H}^{+}: &\quad \{\delta_3(-3\delta_1+\delta_3)^2 = 27a\delta_2^2, \delta_3>0, \delta_1<\delta_3, -\delta_1>\delta_3, a\neq 0\},\\ \boldsymbol{DH}: &\quad \{27a\delta_2^2 = -16\delta_3^3, \delta_1=\delta_3\}. \end{aligned}$$

5.5. **Proof of Theorem 3.1(ii).** Here we study the case $\alpha<0$ in system (12β).

5.5.1. *Local bifurcations of vector field (13)-(14).* Let u_0 be a root of polynomial $f(u)=-au^3+u\delta_1+\delta_2 (a\neq 0)$.

Proposition 4. *Singular point $(u_0,0)$ of vector field (13)-(14) with $\alpha<0$ is*

1) a two-multiple singular point, corresponding to the fold bifurcation if $u_0^2=\delta_1/(3a)$, $u_0\neq 0$, $\delta_1\neq\delta_3$,

2) a neutral spiral,[2] *corresponding to the Andronov-Hopf bifurcation if $u_0^2=\delta_3/(3a)$, $\delta_3<\delta_1$;*

3) a three-multiple singular point, corresponding to the cusp bifurcation if $\delta_1=\delta_2=0$ and $\delta_3\neq 0$; and

4) a degenerate saddle corresponding to the Bogdanov-Takens bifurcation, if $3au_0^2=\delta_1=\delta_3$ and $u_0\neq 0$.

Proof. Let us shift the point $(u_0,0)$ to the origin:

$$v=u-u_0 \Rightarrow u=v+u_0 \Rightarrow u'=v'.$$

Then system (13)-(14) takes the form

$$v'=z,\ z'=Q(v,z) \tag{25}$$

where $Q(v,z)=a_{10}v+a_{01}z+a_{20}v^2+a_{02}z^2+a_{11}zv+a_{12}vz^2+a_{21}v^2z+a_{30}v^3+a_{03}z^3$, and coefficients $a_{ij}(i,j=1,2,3)$:

$$\begin{aligned} a_{10} &= \alpha(\delta_1-3au_0^2), a_{01}=\alpha(\delta_3-3au_0^2), \quad (26)\\ a_{20} &= -3\alpha a u_0, a_{02}=-3\alpha a u_0, a_{11}=-6\alpha a u_0,\\ a_{30} &= -\alpha a, a_{21}=-3\alpha a, a_{12}=-3\alpha a, a_{03}=-\alpha a. \end{aligned}$$

The proof of the Proposition uses the following statements.

Lemma 5.2. [38]. *Singular point O of vector field (25) is*

1) a two-multiple singular point, corresponding to the fold bifurcation if $a_{10}=0$, $a_{01}a_{20}\neq 0$;

2) a neutral spiral, corresponding to the Andronov-Hopf bifurcation if $a_{01}=0$, $a_{10}<0$ and the first Lyapunov value $L_1\equiv -A(a_{11}(-a_{20}+a_{10}a_{02})+a_{10}(-3a_{10}a_{03}+a_{21}))\neq 0$, where A is a positive constant;

3) a three-multiple singular point, corresponding to the cusp bifurcation, if $a_{10}=0$, $a_{20}=0$, and $a_{01}a_{30}\neq 0$; and

4) a degenerate saddle corresponding to the Bogdanov-Takens bifurcation if $a_{01}=0$, $a_{10}=0$, and $a_{11}a_{20}\neq 0$.

Statements 1, 3, and 4 of Proposition 4 follow from the corresponding statements 1, 3, and 4 of Lemma 5.2 by direct substitution of coefficients (26). Let us prove statement 2 of Proposition 4. If $a_{01}=0$, then $u_0^2=\delta_3/3a$; if $\alpha a_{10}<0$, then $a_{10}>0$, which implies $\delta_1-3au_0^2>0$, hence $\delta_1>\delta_3>0$. So the first Lyapunov quantity $L_1\cong 3a\alpha^2(\delta_3+\delta_1)(\alpha(\delta_3-\delta_1)+1)$ is positive for $\delta_1>\delta_3>0$, $\alpha<0$, and any δ_2.

Proposition 4 is proved.

[2] A neutral spiral is a singular point having imaginary eigenvalues

Corollary 2. *For system (13)-(14) with $\alpha < 0$ the boundaries of the parameter portrait corresponding to the fold, cusp and Bogdanov-Takens bifurcations are given by the equations (22). The boundary corresponding to the subcritical Andronov-Hopf bifurcations is* $\boldsymbol{H}$: $\{\delta_3(-3\delta_1+\delta_3)^2 = 27a\delta_2^2, \delta_1 > \delta_3 > 0, a \neq 0\}$.

5.5.2. *Homo/heteroclinic nonlocal bifurcations.* The parametric portrait for the Bogdanov-Takens bifurcation contains a boundary $\boldsymbol{P}$ of the homoclinic bifurcation. System (13)-(14) with $\alpha < 0$ has two non-local homoclinic bifurcations; they correspond to the boundaries $\boldsymbol{P}^1$ and $\boldsymbol{P}^2$ at the portrait given in Figure 4a. In more detail, the system has two Bogdanov-Takens bifurcations, see points $\boldsymbol{BT}_1$ and $\boldsymbol{BT}_2$ in Figure 4a, which are the points of intersection of the Hopf boundaries $\boldsymbol{H}$ with fold boundaries $\boldsymbol{S}_1$ and $\boldsymbol{S}_2$ (see [1], [16], [24]).

Let us reduce system (13)-(14) to the generalized Lienard form by scaling (20)-(21) with $\alpha \to -\alpha$:

$$y_1' = y_2,\ y_2' = h(y_1) + y_2 r(y_1) + y_2^2\varphi(y_1, y_2) \tag{27}$$

where $h(y_1) = \mu_2 + \mu_1 y_1 + y_1^3, r(y_1) = (\mu^3 + y_1^2), \varphi(y_1, y_2) = \dfrac{y_1}{3} + \dfrac{y_2}{27}$, and

$$\mu_2 = 27a^{1/2}(-\alpha)^{1/2}\alpha\delta_2, \mu_1 = 9\alpha\delta_1, \mu_3 = 3\alpha\delta_3. \tag{28}$$

Due to assertions (A) and (B) from Section 5.3, system (27) is topologically equivalent to the system

$$y_1' = y_2,\ y_2' = h(y_1) + y_2 p(y_1),\ p(y_1) = \mu_3 + \mu_4 y_1 + \nu y_1^2 \tag{29}$$

for small values of μ_1, μ_2, and μ_3 with $\mu_4 = 0$ and $\nu \neq 0$.

The following results are known for heteroclinic bifurcations of system (29):

(i) For $\mu_4 \neq 0$ and $\nu = 0$ the equations for boundary surfaces $\boldsymbol{L}^1$, $\boldsymbol{L}^2$ were derived in [4];

(ii) For $\mu_4 \neq 0$ and $\nu = \pm 1$ the surfaces $\boldsymbol{L}^1$, $\boldsymbol{L}^2$ exist ([10]); and

(iii) For $\mu_4 \neq 0$ and $\mu_2 = 0$ system (29) is Z_2-equivariant; in this case the existence of $\boldsymbol{L}^1$, $\boldsymbol{L}^2$ has been proved and the equation $\mu_3 = \mu_1/5 + o(\mu_1),\ \mu_1 < 0$ of the line of intersection of surfaces $\boldsymbol{L}^1$, $\boldsymbol{L}^2$, $\boldsymbol{P}^1$ and $\boldsymbol{P}^2$ was found in [22] (see also [1]).

In the case $\mu_4 = 0$ we explored system (29) numerically using program packages [26], [21]; for $\nu = 1$ and various parameter points μ_1, μ_2, μ_3 we observed separatrix connections of saddle points of the system corresponding to $\boldsymbol{L}^1$, $\boldsymbol{L}^2$.

Recall that $\mu_1 = 9\alpha\delta_1$, $\mu_3 = 3\alpha\delta_3$ and $\alpha < 0$, so $\delta_1 > 0$, $\delta_3 > 0$ at the line of intersection of $\boldsymbol{L}^1$, $\boldsymbol{L}^2$ for the case $\mu_2 = 0$.

Next, the divergence of vector field (29) for $\nu = 1$ and $\mu_4 = 0$ is positive, $\mathrm{div}J = (\mu_3 + y_1^2) > 0$ for $\mu_3 > 0$. Hence, vector field (13)-(14) with $\alpha < 0$ has no closed orbits and separatrix loops for any $\delta_3 < 0$ because $\mu_3 = 3\alpha\delta_3 > 0$. The heteroclinics exist for any δ_3 but corresponding boundaries $\boldsymbol{L}^1$, $\boldsymbol{L}^2$ intersect only for $\delta_3 > 0$. As a result of the performed analysis we obtained heteroclinic boundaries $\boldsymbol{L}^1$, $\boldsymbol{L}^2$ presented in Figures 4a and 4b.

5.5.3. *On limit cycles.* The bifurcation diagram of the Bogdanov-Takens bifurcation contains the parameter domain, which has a single phase limit cycle (see [6], [1]). Recall that this cycle is unstable because the Andronov-Hopf bifurcation at $\boldsymbol{H}$ is subcritical. System (12−) has two $\boldsymbol{BT}$ bifurcations hence the parameter portrait contains two domains of phase limit cycles (see Figures 4a and 5).

Next, the blow-up scaling

$$y_1 \to \delta y_1, \qquad y_2 \to \delta^2 y_2, \qquad \mu_1 \to \delta^2 \mu_1,$$
$$\mu_2 \to \delta^3 \mu_2, \qquad \mu_3 \to \delta^3 \mu_3, \qquad t \to t/\delta \quad \text{with } \delta > 0$$

transforms vector field (29) to the vector field with

$$h(y_1) = \mu_2 + \mu_1 y_1 + y_1^3, \qquad r(y_1) = \delta(\mu_3 + y_1^2). \tag{30}$$

System (29), (30) can be considered as a small perturbation of the Hamiltonian system for $\delta = 0$. The necessary condition for the appearance of limit cycles or homo/heteroclinic loops from corresponding closed ovals or loops γ of the Hamiltonian system is

$$\oint_\gamma (\mu_3 + y_1^2) y_2 dy_1 = 0. \tag{31}$$

Analysis of equation (31) with the help of well developed methods (see [8], [10], [36]) allowed us to state that for small positive δ a limit cycle exists and coincide with the limit cycle, which was observed in domains 4 of the parameter portrait (see, Figures 4a and 5).

5.6. **Description of nonlocal bifurcations of the vector-fields (18), (19).** Let us describe boundaries in the parameter space $\{\delta, \alpha\} = \{\delta_1, \delta_2, \delta_3, \alpha\}$ corresponding to non-local bifurcations of vector field $\boldsymbol{J}$. For *positive* α there exist the following bifurcation surfaces (at $\delta_3 > 0$, see Fig. 2a).

The bifurcation "two-multiple cycles" is realized on the surface $\boldsymbol{D}$, which touches the surfaces $\boldsymbol{H}_1$, $\boldsymbol{H}_2$ by lines $\boldsymbol{DH}_1$, $\boldsymbol{DH}_2$, respectively.

The bifurcation "a *small* loop composed by one of separatrix pairs of the saddle point" is realized on the surfaces $\boldsymbol{P}_1$, $\boldsymbol{P}_2$ and "a *large* loop composed by one of separatrix pairs of the saddle point" is realized on the surfaces $\boldsymbol{R}_1$, $\boldsymbol{R}_2$. Surfaces $\boldsymbol{S}_1$, $\boldsymbol{H}_1$ and $\boldsymbol{P}_1$ have common lines $\boldsymbol{BT}_1$ (see Fig. 2a) as well as $\boldsymbol{S}_2$, $\boldsymbol{H}_2$ and $\boldsymbol{P}_2$ have common lines $\boldsymbol{BT}_2$ [6]. Surfaces $\boldsymbol{R}_1$, $\boldsymbol{R}_2$ have common lines of touching with surfaces $\boldsymbol{S}_1$, $\boldsymbol{S}_2$. The intersection of $\boldsymbol{R}_1$, $\boldsymbol{R}_2$ (see Fig. 2) corresponds to the phase portrait, which contains a saddle whose four separatrices compose "8"; this bifurcation was studied in [33].

For negative α there exist the following bifurcation surfaces (at $\delta_3 > 0$, see Fig. 4a).

The bifurcation "a small loop composed by one of separatrix pairs of the saddle point" is realized on the surfaces $\boldsymbol{P}^1$, $\boldsymbol{P}^2$. Surfaces $\boldsymbol{S}_1$, $\boldsymbol{H}$ and $\boldsymbol{P}^1$ have common lines $\boldsymbol{BT}_1$ as well as $\boldsymbol{S}_2$, $\boldsymbol{H}$ and $\boldsymbol{P}^2$ have common lines $\boldsymbol{BT}_2$.

The bifurcation "upper, lower (respectively) heteroclinics of saddle singular points" is realized on the surfaces $\boldsymbol{L}^1$, $\boldsymbol{L}^2$ as for $\delta_3 > 0$ so for $\delta_3 < 0$. For $\delta_3 > 0$, $\boldsymbol{L}^1$, $\boldsymbol{L}^2$ and $\boldsymbol{P}^1$, $\boldsymbol{P}^2$ have a common line of intersection [36] such that two heteroclinics simultaneously join saddle points.

Acknowledgments. FB appreciates Dr. C. Castillo-Chavez and Dr. S. Baer for numerous useful discussions.

REFERENCES

[1] V. I. Arnold, *Geometrical methods in the theory of ODE*, Springer-Verlag, 1983.

[2] G. Belitskii, *Equivalence and normal forms of germs of smooth mappings*, Russian Mathematical Surveys **33** (1978), 95-155.

[3] F. S. Berezovskaya, *About solutions "traveling waves" of Lienard' equation cross-diffusion updating*. Abstracts of ICM-98, Berlin, (1998), 198.

[4] F. Berezovskaya and G. Karev, *Bifurcations of traveling waves in population models with taxis*. Physics-Uspekhi **42** (1999), 917-29.
[5] F. S. Berezovskaya and G. P. Karev, *Equations with cross-diffusion as the models of populations with attractant*. Biophysics **45** (2000), 732-37.
[6] R. I. Bogdanov, *Versal deformation of a singular point on the plane in the case of zero eigenvalues*, in "Proceedings of Petrovskii Seminar, v.2", Moscow University, 37-65 (In Russian); English translation: Selecta Math. Soviet. **1** (1976), 373-88.
[7] J. H. E. Cartwright, E. Hermandez-Garcia, and O. Piro, *Burridge-Knopoff models as elastic excitable media*. Phys. Rev. Lett. **79** (1997), 527-30.
[8] G. Dangelmayr and J. Guckenheimer, *On a four parameter family of planar vector fields*, Arch. Ration. Mech. **97** (1987), 321-52.
[9] B. Deng, *The existence of infinite traveling front and back waves in FitzHugh-Nagumo equation*, SIAM J.Math. Anal. **22** (1991), 1631-50.
[10] F. Dumortier, R. Rossarie, and J. Sotomayor, *Bifurcations of planar vector fields*, Lect. Notes in Mathematics **1480** (1991), 1-164.
[11] J. Evans, N. Fenichel, and J. Feroe, *Double impulse solutions in nerve axon equations*, SIAM J.Appl. Math. **42** (1982), 219-34.
[12] R. FitzHugh, *Impulses and physiological states in theoretical models of nerve membrane*. Biophys. J. **1** (1961), 445-66.
[13] R. FitzHugh, *Mathematical Models of Excitation and Propagation in Nerve*, in "Biological Engineering" (ed. H. P. Schwan), McGraw-Hill, (1969), 185.
[14] R. Franca, I. Prendergast, E. Sanchez, M. A. Sanchez, and F. Berezovsky, *The Role of Time Delay in the FitzHugh-Nagumo Equations: The Impact of Alcohol on Neuron Firing*, Cornell University Biometrics Department Technical Report, **BU-1577-M** (2001), 3-31.
[15] R. A. Gubitosi-Klug and R. W. Gross, *Nonoxidative Metabolites of Ethanol, Accelerate the Kinetics of Activation of the Human Brain Delayed Rectifier K1 Channel, Kv1.1*, J. Biol. Chem. **271** (1996), 32519-22.
[16] J. Guckenheimer and P. Holmes, *Nonlinear oscillations, dynamical systems, and bifurcations of vector fields*, Springer-Verlag, 1983.
[17] S. Hastings, *On the existence of homoclinic and periodic orbits for the FitzHugh-Nagumo equations*. Quart. J. Math. (Oxford) **27** (1976), 123-34.
[18] R. Highfield, *The brains teasing chemical cocktail that gets us drunk*. UK News, Electronic Telegraph, Issue 582, 1996.
[19] A. L. Hodgkin and A. F. Huxley, *A quantitative description of membrane current and its application to conduction and excitation in nerve*, J. Physiol. **117** (1952), 500-44.
[20] A. Khibnik, B. Krauskopf, and C. Rousseau, *Global study of a family of cubic Lienard equations*, Nonlinearity **11** (1998), 1505-19.
[21] A. I. Khibnik, Y. A. Kuznetsov, V. V. Levitin, and E. V. Nikolaev, *Continuation techniques and interactive software for bifurcation analysis of ODEs and iterated maps*, Physica D, **62** (1993), 360-371.
[22] E. Khorozov, *Versal deformations of equivariant vector fields for the case of symmetries of orders 2 and 3*. Topics of modern mathematics (Petrovskii Seminar), **5** (1985), 207-243.
[23] T. Kostova, R. Ravindran, M. Schonbek, *FitzHugh-Nagumo Revisited: Types of Bifurcations, Periodical Forcing and Stability Regions by Lyapunov Functional*, Int. Journal of Bifurcation and Chaos, **14**:3 (2004), 913-926.
[24] Y. A. Kuznetsov, *Elements of applied bifurcation theory*, Springer-Verlag, 1997.
[25] Y. A. Kuznetsov, M. Y. Antonovsky, V. N. Biktashev, and E. A. Aponina, *A cross-diffusion model of forest boundary dynamics*, J.Math.Biol. **32** (1994), 219-35.
[26] V. Levitin, *TRAX: Simulation and Analysis of Dynamical systems*, NY: Exeter Publishing, 1987.
[27] J. D. Murray, *Mathematical Biology*, Springer-Verlag, 1993.
[28] J. Nagumo, S. Arimoto, and S. Yoshisawa, *An active pulse transmission line simulating nerve axon*, Proc. IRE **50** (1962), 2061-70.
[29] A. Nogaret, N. J. Lambert, S. J. Bending, and J. Austin, *Artificial ion channels and spike computation in modulation-doped semiconductors*, Europhys. Lett. **68** (2004), 874-80.
[30] V. V. Osipov, Noise in physical systems, SOV PHYS USPEKHI **33** (1990), 1081-82.
[31] H. G. Othmer and A. Stevens, *Aggregation, Blow-up and Collapse: the Abcs of Taxis in Reinforced Random Walks*, SIAM J. of Appl. Math. **57** (1997), 1044-81.

[32] F. Sanchez-Garduno and P. K. Maini, *Travelling wave phenomena in non-linear diffusion degenerate Nagumo equations*, J.Math.Biol. **35** (1997), 713-28.
[33] B. Sanstede, *Stability of N-fronts bifurcating from a twisted heteroclinic loop and an application to the FitzHugh-Nagumo equations*, SIAM J. Math. Anal. **29** (1998), 183-207.
[34] L. Sherwood, *Human Physiology: From Cells to Systems*, 4th edition, Brooks and Cole Publishers, 2001.
[35] F. Takens, *Normal forms for certain singularities of vector fields*, Ann. Inst. Fourier, Grenoble **23** (1973), 163-95.
[36] D. Turaev, *Bifurcations of two-dimensional dynamical systems close to those possessing two separatrix loops*. Mathematics survey **40** (1985), 203-04.
[37] D. W. Verzi, M. B. Rheuben, and S. M. Baer, *Impact of time-dependent changes in spine density and spine change on the input-output properties of a dendric branch: a computational study*, J. Neurophysiol. **93** (2005), 2073-89.
[38] E. P. Volokitin and S. A. Treskov, *Parameter portrait of FitzHugh system Mathematical modeling*, (In Russian) **6** (1994), 65-78.
[39] A. I. Volpert, V. A. Volpert, and V. A. Volpert, *Traveling wave solutions of parabolic systems*, AMS, Providence, 1994.
[40] N. Wei-Ming, *Diffusion, cross-diffusion and their spike-layer steady states*, Notices Amer. Math. Soc. **45** (1998), 9-18.

Received on May 8, 2007. Accepted on January 29, 2008.

E-mail address: fsberezo@hotmail.com
E-mail address: email2@aimSciences.org